



## 저작자표시-비영리-변경금지 2.0 대한민국

이용자는 아래의 조건을 따르는 경우에 한하여 자유롭게

- 이 저작물을 복제, 배포, 전송, 전시, 공연 및 방송할 수 있습니다.

다음과 같은 조건을 따라야 합니다:



저작자표시. 귀하는 원저작자를 표시하여야 합니다.



비영리. 귀하는 이 저작물을 영리 목적으로 이용할 수 없습니다.



변경금지. 귀하는 이 저작물을 개작, 변형 또는 가공할 수 없습니다.

- 귀하는, 이 저작물의 재이용이나 배포의 경우, 이 저작물에 적용된 이용허락조건을 명확하게 나타내어야 합니다.
- 저작권자로부터 별도의 허가를 받으면 이러한 조건들은 적용되지 않습니다.

저작권법에 따른 이용자의 권리는 위의 내용에 의하여 영향을 받지 않습니다.

이것은 [이용허락규약\(Legal Code\)](#)을 이해하기 쉽게 요약한 것입니다.

[Disclaimer](#)

The development of long non-coding  
RNA *HOTAIR* as a serum biomarker  
in cervical cancer by Notch targeting  
pathway

Maria Lee

Department of Medicine

The Graduate School, Yonsei University

The development of long non-coding  
RNA *HOTAIR* as a serum biomarker  
in cervical cancer by Notch targeting  
pathway

Maria Lee

Department of Medicine

The Graduate School, Yonsei University

The development of long non-coding  
RNA *HOTAIR* as a serum biomarker  
in cervical cancer by Notch targeting  
pathway

Directed by Professor Young Tae Kim

The Doctoral Dissertation  
submitted to the Department of Medicine,  
the Graduate School of Yonsei University  
in partial fulfillment of the requirements for the degree  
of Doctor of Philosophy

Maria Lee

June 2016

This certifies that the Doctoral  
Dissertation of Maria Lee  
is approved.

-----  
Thesis Supervisor: Young Tae Kim

-----  
[Thesis Committee Member#1: Yong Sang Song]

-----  
[Thesis Committee Member#2: Nam Hoon Cho]

-----  
[Thesis Committee Member#3: Sang Wun Kim]

-----  
[Thesis Committee Member#4: Kyung-Hee Chun]

The Graduate School  
Yonsei University

June 2016

## ACKNOWLEDGEMENTS

I would like to express profound gratitude to my supervisor, Professor Young Tae Kim, for his invaluable support, encouragement, supervision and useful suggestions throughout this research work. His moral support and continuous guidance enabled me to complete my work successfully. I am also highly thankful to Professor Yong Sang Song, Nam Hoon Cho, Sang Wun Kim and Kyung-Hee Chun for their valuable suggestions throughout this study. I would like to thank Hee Jung Kim for valuable advices in science discussion and guidance from the early stage of this research.

I am as ever, especially indebted to my parents and sister for their love and support throughout my life. They always had only new ways of supporting and encouraging me on, even during some difficult moments. They have been my inspiration and motivation throughout this work.

Maria Lee

## <TABLE OF CONTENTS>

ABSTRACT.....	1
I. INTRODUCTION.....	3
II. MATERIALS AND METHODS.....	5
1. Patient and sample collection.....	5
2. Cell culture.....	5
3. Plasmid constructs and the generation of stable cell line.....	6
4. Small interfering RNA (siRNA) transfection.....	6
5. Quantitative real-time PCR analysis (qPCR).....	6
6. Western blot analysis.....	8
7. Xenografts in Mice.....	9
8. Magnetic Resonance (MR) Imaging in Mice.....	9
9. Micro Positron Emission Tomography (PET) Imaging in Mice...	10
10. Cell proliferation assay.....	10
11. Wound healing assay.....	11
12. Matrigel invasion assay.....	11
13. Statistical Analysis.....	12
III. RESULTS.....	12
1. <i>HOTAIR</i> is elevated in cervical cancer patients and <i>HOTAIR</i> overexpression is associated with poor prognosis.....	12
2. <i>HOTAIR</i> knockdown in cervical cancer cells inhibits cell proliferation and invasion.....	18
3. <i>HOTAIR</i> overexpression promotes cell growth, invasion, and migration.....	19
4. <i>HOTAIR</i> knockdown in cervical cancer cells increases apoptosis .....	21
5. <i>HOTAIR</i> overexpression in SiHa cells increases xenograft tumour growth in mice.....	22

6. <i>HOTAIR</i> promotes a malignant phenotype in cervical cancer cells through the epithelial-mesenchymal transition (EMT) and Notch signalling pathways.....	25
IV. DISCUSSION.....	29
V. CONCLUSION.....	31
REFERENCES.....	32
ABSTRACT (IN KOREAN) .....	36



## LIST OF FIGURES

Figure 1. Elevated expression of <i>HOTAIR</i> in human cervical cancer serum.....	13
Figure 2. Kaplan-Meier curves showing disease-free survival (A) and overall survival (B) of cervical cancer patients according to the <i>HOTAIR</i> expression status.....	18
Figure 3. <i>HOTAIR</i> overexpression promotes cell invasion..	20
Figure 4. Effects of <i>HOTAIR</i> on apoptosis .....	22
Figure 5. Effect of <i>HOTAIR</i> on tumor growth <i>in vivo</i> .....	24
Figure 6. <i>HOTAIR</i> regulates the Notch signalling pathway.	26
Figure 7. <i>HOTAIR</i> overexpression promotes EMT-related gene expression in xenografts .....	27
Figure 8. <i>HOTAIR</i> overexpression promotes the expression Notch pathway genes in xenografts.....	28

## LIST OF TABLES

Table 1. Clinicopathological characteristics of the 153 cervical cancer patients.....	14
Table 2. Univariate and multivariate analyses for determinants of disease free survival.....	16
Table 3. Univariate and multivariate analyses for determinants of overall survival .....	17

## &lt;ABSTRACT&gt;

**The development of long non-coding RNA *HOTAIR* as a serum biomarker in cervical cancer by Notch targeting pathway**

Maria Lee

*Department of Medicine  
The Graduate School, Yonsei University*

(Directed by Professor Young Tae Kim)

*HOTAIR* is a long non-coding RNAs (lncRNA) that plays a role as an oncogenic molecule in cervical cancer. In this study, we investigated in detail the expression of serum *HOTAIR*, as well as its functions, in cervical cancer. Serum *HOTAIR* expression was assessed by qRT-PCR and the results were compared with clinicopathologic factors, including survival data. The effects of *HOTAIR* overexpression via lentiviral transfection were examined in SiHa cells and a xenograft model. The expression of *HOTAIR* in cervical cancer serum was significantly higher than in the control groups ( $P < 0.001$ ), and this increase of expression was significantly associated with tumor size ( $P = 0.030$ ), lymphovascular space invasion ( $P = 0.037$ ), and lymph node metastasis ( $P = 0.043$ ). In univariate analysis, disease free survival and overall survival in cervical cancer was significantly shorter in cases with high *HOTAIR* expression (hazard ratio [HR] = 4.27, 4.68 and  $P = 0.039$ , 0.031, respectively). *HOTAIR* overexpression in cervical cancer cells resulted in increase of cell proliferation and invasion *in vitro*, whereas *HOTAIR* knockdown inhibited these properties and increased apoptosis. In addition, *in vivo* experiments using *HOTAIR* overexpression clearly showed a strong inducer of tumor growth and a modulation of expression of epithelial-mesenchymal transition and Notch

signaling pathway related genes, further suggesting that *HOTAIR* overexpression can promote cell proliferation and invasion. Taken together, increased serum *HOTAIR* expression is associated with poor survival outcome in cervical cancer, and *HOTAIR* may represent a useful therapeutic target in cervical cancer patients.

---

Key words: cervical cancer; long non-coding RNA; *HOTAIR*; lentivirus; Notch

**The development of long non-coding RNA *HOTAIR* as a serum  
biomarker in cervical cancer by Notch targeting pathway**

Maria Lee

*Department of Medicine  
The Graduate School, Yonsei University*

(Directed by Professor Young Tae Kim)

## **I. INTRODUCTION**

In 2012, cervical cancer was ranked fourth in incidence and mortality among female cancers worldwide. Globally, cervical cancer had an estimated 528,000 new cases and was responsible for 266,000 deaths in 2012.<sup>1</sup> Recently, the decreased incidence and mortality rates in developed countries have been attributed to the effectiveness of the screening test for cervical cancer. However, the incidence rate remains high in developing countries, where it accounts for 85% of all cervical cancer cases.<sup>2</sup> The cure rate of cervical cancer is up to 80-90% in the early stages (Stages I-II), and 60% in Stage III. However, the prognosis is still poor with cancer progression to an advanced stage or recurrence.

Most recently, data have shown that circulating non-coding RNAs are emerging as a novel class of diagnostic or prognostic biomarkers for malignant tumors.<sup>3,4</sup> Previous studies have indicated that lncRNAs exist in human body fluids<sup>5,6</sup> and have revealed their potential utility as diagnostic biomarkers.<sup>7</sup> But little is known about whether circulating lncRNAs can serve as biomarkers in

cervical cancer. HOX transcript antisense RNA (*HOTAIR*) is a well-characterized lncRNA expressed by the human HOXC locus on chromosome 12q 13.13, and it recruits the PRC2 complex to specific target genes in the HOXD locus, leading to epigenetic silencing of metastasis suppressor genes.<sup>8</sup> Increased levels of *HOTAIR* have been reported in cervical cancer in the advanced stage, and *HOTAIR* has been found to be a predictor for metastasis and death in cervical cancer patients.<sup>9-11</sup>

However, the studies mainly focused on miRNAs expressed in tumour tissues and cells. Although tissue miRNAs can provide an accurate diagnosis for various types of cancer including cervical cancer, collecting tissue samples is an invasive procedure and depends on surgical sections after the initial clinical classification. Recently, serum and plasma miRNAs have emerged as potential new blood-based markers for detecting cancers and other diseases.<sup>12-15</sup> However, it is unclear whether circulating *HOTAIR* is a potential biomarker for cervical cancer and the role of *HOTAIR* in cervical cancer development and its underlying molecular mechanisms. We have previously identified *HOTAIR* to be upregulated in cervical cancer. However, it is unclear whether circulating *HOTAIR* is a potential biomarker for cervical cancer and the role of *HOTAIR* in cervical cancer development and its underlying molecular mechanisms.

In this study, we found interesting results that the expression of serum *HOTAIR* increased in cervical cancer and high serum *HOTAIR* expression is associated with overall survival in cervical cancer patients. In addition, *HOTAIR* overexpression resulted in increasing of tumor growth via Notch signaling pathway in SiHa cells. Finally, these results suggested that *HOTAIR* plays a crucial role of cancer growth in cervical cancer.

## **II. MATERIALS AND METHODS**

### **1. Patient and sample collection**

Blood serum samples were obtained from 153 female patients who underwent surgery at Yonsei Severance Hospital, Yonsei University, between 2007 and 2012. All the sera from patients with newly diagnosed invasive cervical cancer who had not received prior treatment were included in the study. Eighty samples were chosen from patients undergoing simple hysterectomy because of uterine leiomyoma were obtained as controls. Samples from patients with concomitant gynecological cancer were excluded from the study.

The serum from patients and controls was obtained by using the same collection and sampling procedures as follows: 4 ml peripheral blood was sampled in BD Vacutainer tubes and incubated at room temperature from 30 to 60 min, and then centrifuged at 2000 rpm for 15 min at room temperature. The supernatant was transferred to an EP tube and stored at -80°C until RNA extraction. The study was conducted according to the principles in the Declaration of Helsinki and was approved by the ethical committee of Yonsei Severance Hospital. Informed consent was obtained from all patients. The clinical information is summarized in Table 1.

### **2. Cell culture**

SiHa (squamous cervical carcinoma), HeLa (epitheloid cervical carcinoma) and Caski (epidermoid cervical carcinoma established from a metastasis in the small bowel mesentery) human cervical cancer cell lines obtained from the American Type Culture Collection (ATCC, Rockville, MD, USA). SiHa and HeLa cells were cultured in Dulbecco's modified Eagle's

medium (Gibco-BRL, Gaithersburg, MD, USA), and Caski cells were cultured in RPMI-1640 medium (Gibco-BRL, Gaithersburg, MD, USA). The human keratinocyte cell line HaCaT was cultured in RPMI-1640 medium. The culture media were supplemented with 10% (vol/vol) fetal bovine serum and penicillin/streptomycin. The cell lines were maintained at 37°C in a humidified atmosphere of 5% CO<sub>2</sub> and 95% air. Cells with a passage number <20 were used in all experiments.

### **3. Plasmid constructs and the generation of stable cell line**

The human *HOTAIR* transcript variant 3 cDNA was amplified by PCR and was inserted into the pLenti6/V5-D-TOPO vector according to ViraPower™ Lentiviral Expression systems (Invitrogen). Briefly, plasmid was transfected into the 293FT cell line and then lentivirus was infected in desired cell line. Selection of *HOTAIR* stable transfected cells was performed in medium containing blasticidin (Invitrogen).

### **4. Small interfering RNA (siRNA) transfection**

*HOTAIR* siRNA and negative control siRNA (siNC) were purchased from Bioneer (Daejeon, Korea). Cells ( $5 \times 10^4$  cells/well) were seeded into 6-well plates and were transfected with 10 nM siRNA in phosphate-buffered saline (PBS) using the G-Fectin Kit (Genolution Pharmaceuticals Inc., Seoul, Korea) according to the manufacturer's protocol. These siRNA-transfected cells were used in the *in vitro* assays 48 h post-transfection. The target sequences for *HOTAIR* siRNAs were as follows: siRNA, 5'-AAUUCUAAAUUGGGCUGG-3'.

### **5. Quantitative real-time PCR analysis (qPCR)**



Specimens or cell lines using TRIzol® reagent (Invitrogen, Carlsbad, CA, USA), and 2 µg of total RNA was reverse transcribed into first-strand cDNA by using a reverse transcription reagent kit (Invitrogen) according to the manufacturer's protocol. qRT-PCR was performed using the SYBR® Green real-time PCR kit (Toyobo, Co., Ltd., Osaka, Japan) in a 20-µl reaction volume, which contained 10 µl of SYBR-Green master PCR mix, 5 pmole each of forward and reverse primers, 1 µl of diluted cDNA template, and appropriate amounts of sterile distilled water. Conditions for the amplification of genes were as follows: initial denaturation at 95°C for 3 min; 40 cycles of denaturation at 95°C for 15 sec, annealing at 60°C for 60 sec, and elongation at 72°C for 60 sec; and final elongation at 72°C for 5 min. qRT-PCR was performed on the ABI StepOnePlus Real-Time PCR system (Applied Biosystems, Foster City, CA, USA). All quantifications were performed with *U6* as the internal standard. The PCR primer sequences were as follows: *HOTAIR*, 5'-GGTAGAAAAAGCAACCACGAAGC-3' (sense) and 5'-ACATAAACCTCTGTCTGTGAGTGCC-3' (antisense); *E-cadherin*, 5'-ATTCTGATTCTGC TGCTCTTG-3' (sense) and 5'-AGTAGTCATAGTCCTGGTCCT-3' (antisense);  $\beta$ -catenin, 5' TGCAGTTCGCCTTCACTATG-3' (sense) and 5'-ACTAGTCGTGGAATGGCACC-3'(antisense); *vimentin*, 5'-TGGATTCACTCCCTCTGGTT-3'(sense) and 5'-GGTCATCGTGATGCTGAGAA-3' (antisense); *snail*, 5'-GAGGCGGTGGCAGACTAG-3' (sense) and 5'-GACACATCGGTCAGACCAG-3' (antisense); *twist*, 5'-CGGGAGTCCGCAGTCTTA-3' (sense) and 5'-TGAATCTTGCTCAGCTTGTC-3' (antisense); *Notch1*, 5'-GCCGCCTTTGTGCTTCTGTTC-3' (sense) and 5'-CCGGTGGTCTGTCTGGTCGTC -3' (antisense); *HES1*, 5'-TCAACACGACACCGGATAAA-3' (sense) and

5'-TCAGCTGGCTCAGACTTTCA-3' (antisense); p300,  
 5'-GACCCTCAGCTTTTAGGAATCC-3' (sense) and  
 5'-TGCCGTAGCAACACAGTGTCT-3' (antisense);and U6,  
 5'-CTCGCTTCGGCAGCACA-3' (sense) and  
 5'-AACGCTTCAGGAATTTGCGT-3'(antisense). Relative gene expression was analyzed using the  $2^{-\Delta\Delta CT}$  method, and the results were expressed as extent of change with respect to control values. qRT-PCR experiments were replicated at least 3 times.

## 6. Western blot analysis

Whole cell lysates were prepared by extracting proteins using a buffer containing 50 mM Tris-HCl (pH 7.5), 1 mM EDTA, 1 mM EGTA, 150 mM NaCl, 1 % Nonidet P-40, 0.1 % sodium dodecylsulphate (SDS), 1 mM  $\text{Na}_3\text{VO}_4$ ,  $1\mu\text{g}/\text{ml}$  leupeptin, and 1 mM freshly added phenylmethylsulfonyl fluoride. The protein concentration was measured using the Bio-Rad Protein Assay Kit (Bio-Rad Laboratories). Equal amounts of protein were resolved by 12 % SDS-polyacrylamide gel electrophoresis (PAGE), blotted onto polyvinylidene difluoride membranes (Millipore, Billerica, MA, USA). Blocked membranes were then incubated with primary antibodies (BCL-2, BAX, APAF, Caspase-9, Caspase-3, PARP, NOTCH1, HES1, or p300 rabbit polyclonal antibodies at a final concentration of 1:1000, Cell Signaling, Beverly, MA, USA;  $\beta$ -actin mouse polyclonal antibodies at a final concentration of 1:1000, Sigma, St. Louis, MO, USA) overnight at 4 °C, washed three times (5 min each) with PBS containing 0.1 % Tween 20, and incubated with a horseradish peroxidase-conjugated secondary antibody (1:2000) for 1h at room temperature. The bands were visualized using an enhanced chemiluminescence system (ECL™; Amersham, Little Chalfont, UK), and band intensities were quantified using the Luminescent Image Analyzer (LAS-4000 mini, Fujifilm, Uppsala,

Sweden).

## **7. Xenografts in Mice**

Sixteen BALB/c mice, age 5 to 6 weeks, were provided by Orient Bio (Seongnam, Korea). They were bred in aseptic conditions and kept at a constant humidity and temperature according to standard guidelines under a protocol approved by Yonsei Medical University. All mice were injected subcutaneously in the dorsal scapula region with 150- $\mu$ L suspension ( $1 \times 10^6$ ) of SiHa cells. The size of the tumor was measured twice a week with calipers, and the volume of tumor was determined using the simplified formula of a rotational ellipsoid ( $\text{length} \times \text{width}^2 \times 0.5$ ). Tumors were harvested 50 days after the end of treatment.

## **8. Magnetic Resonance (MR) Imaging in Mice**

MR imaging was performed using a Bruker Biospec 94/24 USR (9.4T) small animal scanner (Bruker BioSpin MRI, Ettlingen, Germany) with a 35mm diameter birdcage coil. During the MR experiments, mice were placed in a custom-built cradle to immobilize their body.  $T_2$ -weighted images were acquired at the beginning of each imaging session for accurate positioning of the animal inside the magnet bore. The  $T_2$ -weighted images were acquired using the rapid acquisition. They were anesthetized during MR experiment with 1.5% isoflurane and a mixture  $O_2/N_2O$  (1:1) with an output of 0.7L/ min. Respiratory motion was monitored during all the experiment using an air pillow. Mice body temperature was maintained constant with a warm water circulation.

## 9. Micro Positron Emission Tomography (PET) Imaging in Mice

The [ $^{18}\text{F}$ ]-fluorodeoxy-glucose (FDG) image was acquired as a reference to evaluate the agent as a diagnostic and therapy follow-up tracer. The same mouse was then injected with a  $^{124}\text{I}$ -labeled derivative of pyropheophorbide-a, which is an imaging and photodynamic therapy bifunctional agent. Because of the long half-life of the  $^{124}\text{I}$  (4.2d), a longitudinal study (multiple scans over time) was possible with the same mouse and the same agent. The tumor uptake relative to the rest of the body increased over time, indicating that the agent has promising potential as both a therapeutic and a tumor-monitoring agent. After incubation with FDG, cervix tumors were imaged using a microPET scanner (Inveon™ Dedicated PET, Siemens). Acquisition data were reconstructed using iterative reconstruction and segmented attenuation. PET image analyses were performed using standard software (Inveon™ Acquisition workplace). A software module was used for fusion and co-registration of PET and CT data, but if needed partly corrected manually. Fused images were analyzed by placing volumes of interest around the calcified areas.

## 10. Cell proliferation assay

Cell proliferation was measured by Cell Counting Kit-8 (CCK-8) assay (Dojindo Laboratories, Kumamoto, Japan). In brief, cells were seeded at  $2 \times 10^3$  viable cells/well on a 96-well microtiter plates in a final volume of 100  $\mu\text{L}$ /well. Cells were incubated overnight to allow for cell attachment and recovery and were then transfected with siNC or siHOTAIR for 24, 48, 72 and 96 h. CCK-8 solution (10  $\mu\text{L}$ ) was added to each well, and the cells were incubated for an additional 2 h. Absorbance was measured at 450 nm using a microplate reader. The experiment was performed in three replicates.

## **11. Wound healing assay**

Cells were seeded at  $5 \times 10^5$  cells/well in 6-well plates and then pre-incubated for 24 hours before creating a wound across the cell monolayer with a yellow plastic tip. The serum-containing medium was removed, and cells were serum starved for 24 h. When the cell density reached ~100% confluence, an artificial homogeneous wound was created by scratching the monolayer with a sterile 200- $\mu$ l pipette tip. After scratching, the cells were washed with serum-free medium. Images of cells migrating into the wound were captured at 0, 24 and 48 h using a microscope. The assay was performed in triplicate.

## **12. Matrigel invasion assay**

The Matrigel invasion assay was performed using the BD Biocoat Matrigel Invasion Chamber (pore size: 8 mm, 24-well; BD Biosciences, Bedford, MA, USA) according to the manufacturer's protocol. In brief, cells ( $0.5 \times 10^5$  viable cells/well) were seeded in the upper chamber, which was coated with Matrigel (BD Transduction Lab, San Jose, CA), and serum-free medium containing 0.1-10% FBS was added to the lower chamber. After 24 hour of incubation, non-migrating cells were removed from the upper chamber with a cotton swab and the cells present on the lower surface of the insert were stained with Differential Quik Stain Kit (Triangle Biomedical Sciences, Inc., Durham, NC). The number of invading cells was quantified by counting of least six random fields (total Magnification x200 per filter). The experiment was repeated three times.

### 13. Statistical Analysis

SPSS software (standard version 20.0; IBM, Chicago, IL) was used for all statistical analyses. Data are expressed as the mean  $\pm$  standard deviation (SD). The association between *HOTAIR* expression and clinicopathological characteristics was assessed using the Pearson's  $\chi^2$  test, Student's t-test, and Fisher's exact test. We determine the median value (1.5) as the cut off value. The groups were categorized by *HOTAIR* expression status above (high *HOTAIR*) and below (low *HOTAIR*) cut-off value (1.5). Overall survival was analyzed by the Kaplan-Meier method, and the differences between groups were estimated by the log-rank test. Multivariate survival analysis was performed for the significant parameters in the univariate analysis using the stepwise Cox regression model analysis. All statistical tests were two-sided, and  $p < 0.05$  was considered to indicate a statistically significant result.

## III. RESULTS

### 1. *HOTAIR* is elevated in cervical cancer patients and *HOTAIR* overexpression is associated with poor prognosis

We previously observed that the transcription level of *HOTAIR* was upregulated >30-fold in cervical cancer tissues by qRT-PCR. We further evaluated *HOTAIR* expression in serum, serum level of *HOTAIR* also elevated in cancer patients ( $4.20794 \pm 0.89$ ) than in control ( $0.76813 \pm 0.24$ ) (Fig.1).

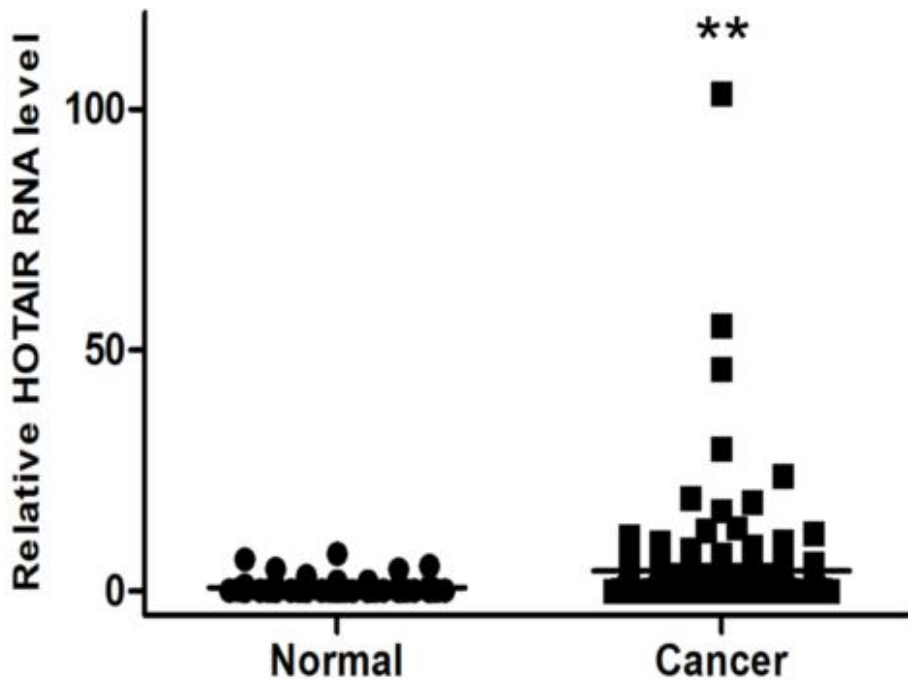


**Figure 1. Elevated expression of *HOTAIR* in human cervical cancer serum**

*HOTAIR* expression was significantly higher in cervical cancer serum (n=153) than in normal serum (n=80). Relative *HOTAIR* expression was determined using qRT-PCR with *U6* as an internal control. Data are expressed as mean  $\pm$  SD. \*\* $P < 0.001$  vs. normal control.

To determine whether circulating *HOTAIR* in serum is linked to clinicopathological features of cervical cancer, we evaluated its relative concentration in the serum of 153 cervical cancer patients at different stages. The average concentration of *HOTAIR* at stage I and II was 4.35 and 3.82, separately, did not showing significant difference in early stage of disease. Serum *HOTAIR* expression was classified into two groups. The groups were categorized by *HOTAIR* expression status above (high *HOTAIR*) and below (low *HOTAIR*) cut-off value (1.5). Clinicopathological data such as age, stage,

histology, tumor size, SCC Ag level, lymphovascular space invasion (LVSI), and lymph node metastasis were analysed between the low and high *HOTAIR* expression groups. Relative high *HOTAIR* expression significantly correlated with features also associated with tumor recurrence, including tumor size ( $P = 0.030$ ), LVSI ( $P = 0.037$ ) and lymph node metastasis ( $P = 0.043$ ) (Table 1).

**Table 1. Clinicopathological characteristics of the 153 cervical cancer patients**

	Frequency	%	Low <i>HOTAIR</i> expression	High <i>HOTAIR</i> expression	P value
<b>Age</b>					0.835
Mean $\pm$ SD	47.6 $\pm$ 11.6		47.4 $\pm$ 11.9	47.7 $\pm$ 11.5	
<b>FIGO Stage</b>					0.413
I	122	79.7	51(83.6)	71(77.2)	
II	29	19.0	9(14.8)	20(21.7)	
III	2	1.3	1(1.6)	1(1.1)	
<b>Cell type</b>					0.711
SCC	113	73.9	44(72.1)	69(75.0)	
AD/ASC	40	26.1	17(27.9)	23(25.0)	
<b>Tumor size</b>					0.030
<4cm	126	82.4	55(90.2)	71(77.2)	
$\geq$ 4cm	27	17.6	6(9.8)	21(22.8)	
<b>SCC Ag level</b>	1.2				0.732
(ng/ml) Median	(0.1	–			
(range)	65.1)				
<b>LVSI</b>					0.037
Negative	95	62.1	31(75.6)	33(54.1)	
Positive	58	37.9	10(24.4)	28(45.9)	



<b>LN metastasis</b>				0.043
Negative	129	84.3	56(91.8)	73(79.3)
Positive	24	15.7	5(9.2)	19(20.7)
<b>Primary</b>				
<b>Treatment</b>				
OP only	94	61.4		
OP + CT	14	9.2		
OP + RT	15	9.8		
OP + CCRT	30	19.6		

FIGO, International Federation of Gynecology and Obstetrics; SCC, squamous cell carcinoma; Ag, antigen; AD, adenocarcinoma; ASC, adenosquamous cell carcinoma; LVSI, lymphovascular space invasion; LN, lymph node; OP, operation; RT, radiotherapy; CCRT, concurrent chemoradiotherapy

We next examined the relationship between *HOTAIR* expression and outcome. Clinicopathological and outcome information was available for 153 cervical cancer patients. The follow-up period of cervical cancer ranged from 1 to 99 months with a mean of 55 months. In univariate analysis, lymphovascular space invasion and high *HOTAIR* status (HR = 6.36,  $P = 0.012$  and HR = 4.27,  $P = 0.039$ , respectively) were prognostic factors of DFS (Table 2, Fig. 2). Kaplan-Meier plots demonstrated that patients with stage II and patients whose tumors were high *HOTAIR* expression displayed significantly worse overall survival ( $P = 0.033$  and  $P = 0.031$ , respectively) (Table 3, Fig. 2). A Cox multivariate proportional hazards analysis showed that lymphovascular space invasion (hazard ratio [HR] = 2.37,  $P = 0.026$ ) was independent prognostic factor of DFS. However, there is no significant prognostic factor of OS.

**Table 2. Univariate and multivariate analyses for determinants of disease free survival**

	Univariate analysis		Multivariate analysis		
	<i>HR</i>	P value	<i>HR</i>	95% CI	P value
Age (< 50 vs. ≥ 50)	0.581	0.446			
FIGO stage (I vs. II)	1.277	0.599			
Histology (SCC vs. AD/ASC)	1.604	0.205			
Tumor size (<4cm vs. ≥4cm)	2.551	0.110			
LVSI	6.355	0.012	2.370	0.109-5.064	0.026
LN metastasis	1.810	0.178			
<i>HOTAIR</i> (low vs. high)	4.269	0.039	1.516	0.661-3.479	0.326

HR, hazard ratio; CI, confidence interval; LN, lymph nodes; FIGO, International Federation of Gynecology and Obstetrics; SCC, squamous cell carcinoma; Ag, antigen; AD, adenocarcinoma; ASC, adenosquamous cell carcinoma; LVSI, lymphovascular space invasion; LN, lymph node

**Table 3. Univariate and multivariate analyses for determinants of overall survival**

	Univariate analysis		Multivariate analysis		
	<i>HR</i>	P value	<i>HR</i>	95% CI	P value
Age (< 50 vs. ≥ 50)	1.091	0.296			
FIGO stage (I vs. II)	4.552	0.033	2.382	0.745-7.622	0.144
Histology (SCC vs. AD/ASC)	7.076	0.008	2.458	0.801-7.540	0.116
Tumor size (<4cm vs. ≥4cm)	3.037	0.081			
LVSI	4.361	0.037	2.631	0.812-8.525	0.107
LN metastasis	10.465	0.001	1.581	0.468-5.339	0.461
<i>HOTAIR</i> (low vs. high)	4.675	0.031	2.733	0.575-12.979	0.206

HR, hazard ratio; CI, confidence interval; LN, lymph nodes; FIGO, International Federation of Gynecology and Obstetrics; SCC, squamous cell carcinoma; Ag, antigen; AD, adenocarcinoma; ASC, adenosquamous cell carcinoma; LVSI, lymphovascular space invasion; LN, lymph node

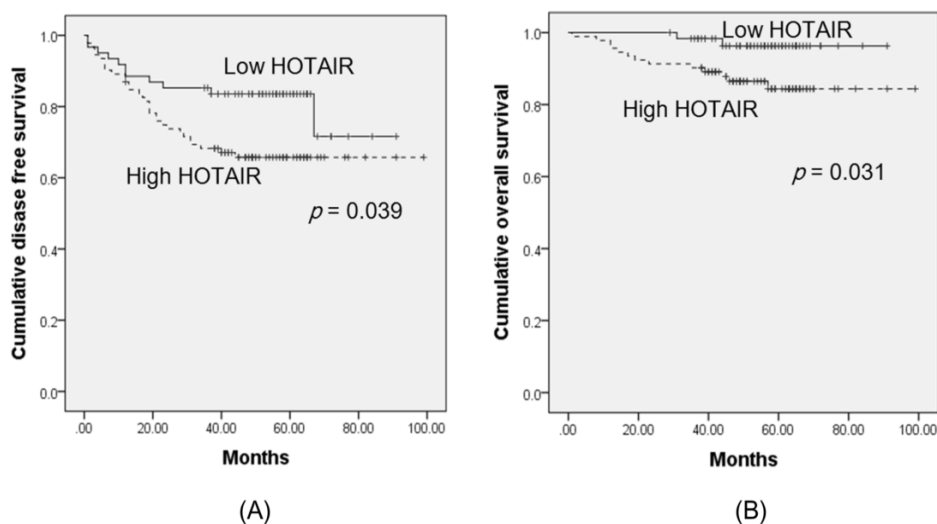


**Figure 2. Kaplan-Meier curves showing disease-free survival (A) and overall survival (B) of cervical cancer patients according to the *HOTAIR* expression status**

## **2. *HOTAIR* knockdown in cervical cancer cells inhibits cell proliferation and invasion**

To determine the functional role of *HOTAIR* in cervical cancer, siRNA was used to downregulate *HOTAIR* expression. In previous our study, *HOTAIR* expression levels were higher in HeLa cells than in SiHa and Caski cells. Therefore, HeLa cells were used for siRNA-mediated knockdown of *HOTAIR* expression.

To determine the role of *HOTAIR* in cervical cancer cell growth, siHOTAIR-transfected cells were used in the CCK-8 assay. siRNA-mediated knockdown of *HOTAIR* decreased cell proliferation by 30% at 96 h post-transfection in HeLa cell. Also, *HOTAIR* siRNA inhibited cell proliferation in SiHa and Caski cells. This finding indicates that *HOTAIR* is involved in the proliferation of cervical cancer cells.

To investigate the effect of *HOTAIR* on migration and invasion, siHOTAIR-transfected cells were used in wound healing and Matrigel invasion assays, respectively. The width of the wound closure was larger in siHOTAIR transfected cells than in siNC-transfected of HeLa, SiHa and Caski cells. Therefore, downregulation of *HOTAIR* decreased the migration of cervical cancer cells. We also tested whether *HOTAIR* knockdown has an inhibitory effect on HeLa cell invasion. Knockdown of *HOTAIR* inhibited HeLa cell invasion >80%.

### **3. *HOTAIR* overexpression promotes cell growth, invasion, and migration**

Next, lentiviral-mediated overexpression of *HOTAIR* was performed to determine the functional role of *HOTAIR* in cervical cancer. Because *HOTAIR* expression is lower in SiHa and CasKi cells than in HeLa cells, SiHa and CasKi cells were used for the overexpression of *HOTAIR*. Following lentiviral-mediated overexpression, *HOTAIR* was upregulated in SiHa, and CasKi cells (Fig. 3A), which significantly enhanced colony formation and cell invasion (Fig. 3B). Also, *HOTAIR* overexpression in SiHa and CasKi cells promoted cell migration (Fig. 3C).

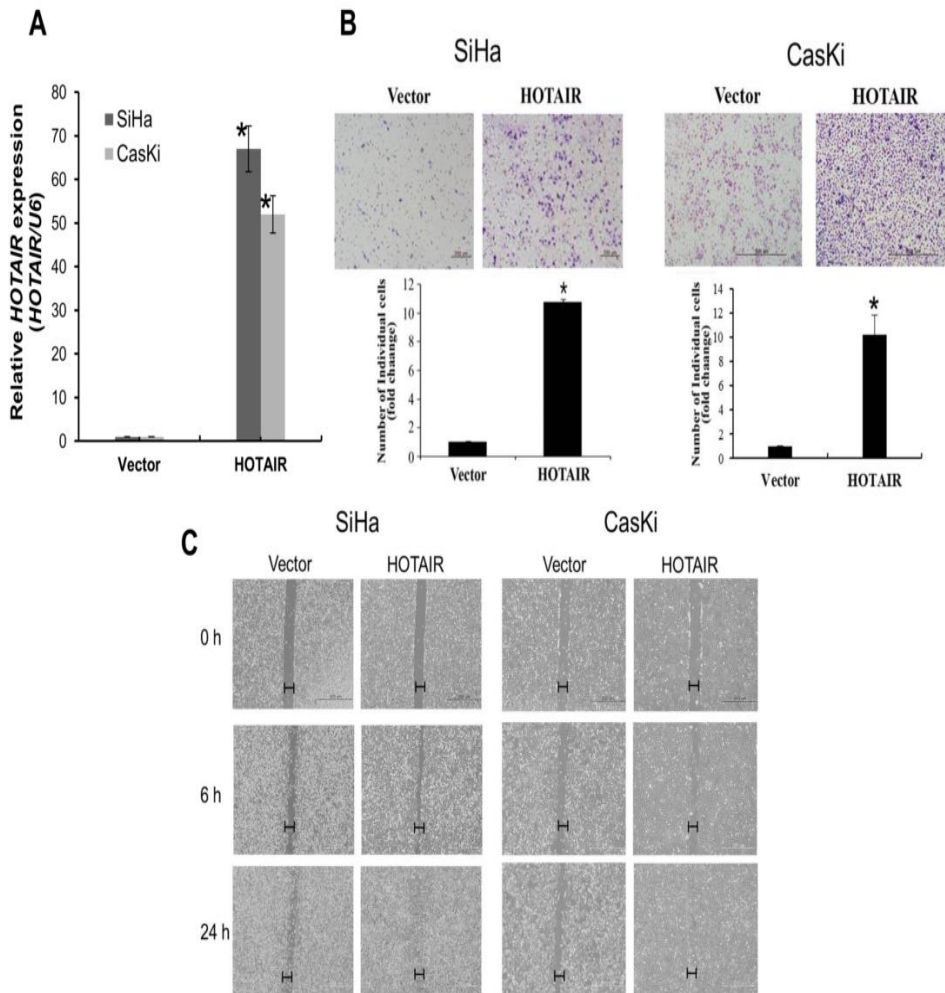
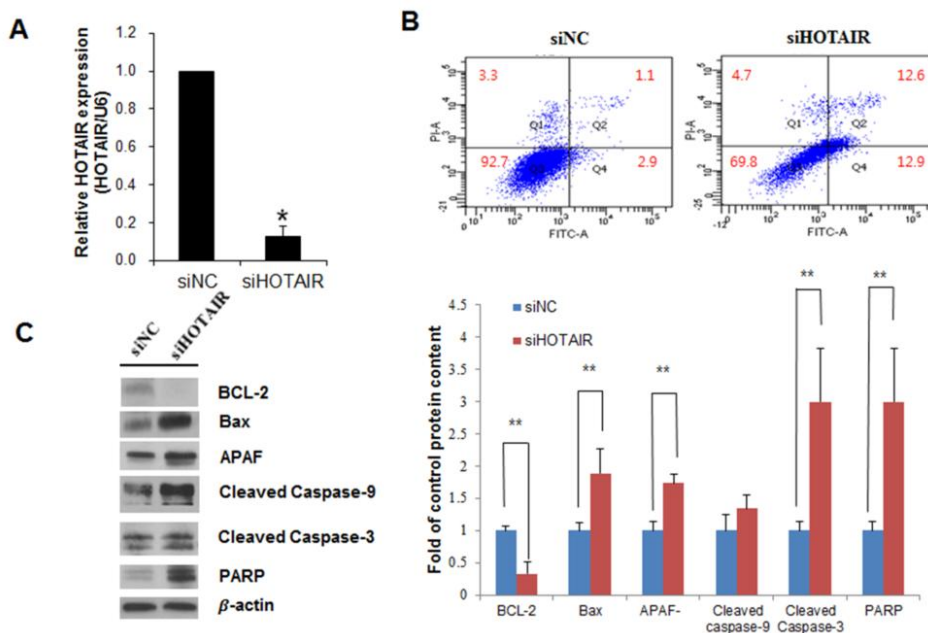


**Figure 3. *HOTAIR* overexpression promotes cell invasion and migration**

(A) Overexpression of *HOTAIR* in SiHa and CasKi cells analysed by qRT-PCR. (B) Using Matrigel invasion chamber, overexpression of *HOTAIR* in SiHa and CasKi cells increased the invasive capacity after 48 h. (C) Wound healing assay was used to determine migration in *HOTAIR* overexpressed cell lines (magnification, x200). Each assay was performed in triplicate. \* $P < 0.05$  vs. control.

#### 4. *HOTAIR* knockdown in cervical cancer cells increases apoptosis

To determine the functional role of *HOTAIR* in cervical cancer, siRNA was used to downregulate *HOTAIR* expression. Flow cytometry was used to detect the percentage of apoptotic cells in siHOTAIR-transfected SiHa cells and overexpression of *HOTAIR* in SiHa cells. *HOTAIR* expression levels decreased in siHOTAIR-transfected SiHa cells (Fig. 4A). As shown in Fig. 4B, knockdown of *HOTAIR* induced apoptosis in SiHa cells (NC 3% vs. siHOTAIR 25.5%). Furthermore, *HOTAIR* knockdown showed downregulation of anti-apoptotic protein Bcl-2 and upregulation of pro-apoptotic protein Bax, Apoptotic protease activating factor (APAF), caspase-9, caspase-3 and Poly (ADP-ribose) polymerase (PARP) (Fig. 4C). These results demonstrated that *HOTAIR* knockdown significantly increased apoptosis in SiHa cells. On the other hand, overexpression of *HOTAIR* in SiHa cells decreased apoptosis (Fig. 4D, 4E).



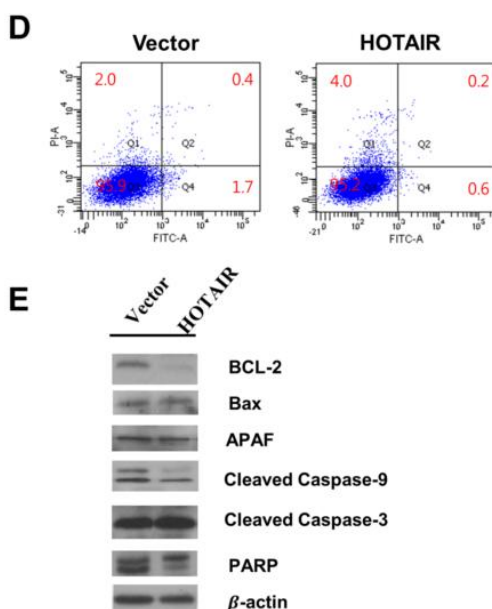


**Figure 4. Effects of *HOTAIR* on apoptosis**

(A) Cells were transfected with *HOTAIR*-specific siRNA and negative control siRNA, and knockdown efficacy was determined by qRT-PCR analysis. (B) Apoptosis were measured using Annexin V/PI staining in *HOTAIR* silencing SiHa cells. *HOTAIR* silencing enhanced the apoptosis. (C) Western blot analysis of apoptosis related proteins BCL-2, Bax, APAF, caspase-9, cleaved caspase-3, PARP in SiHa cells. Band intensities were quantified and normalized to that of  $\beta$ -actin. \* $P < 0.05$ , \*\* $P < 0.01$  vs. control. (D) Apoptosis were measured using Annexin V/PI staining and (E) western blotting in overexpression of *HOTAIR* in SiHa cells.

## 5. *HOTAIR* overexpression in SiHa cells increases xenograft tumour growth in mice

To explore whether *HOTAIR* can affect tumour growth *in vivo*, we inoculated SiHa cells as xenografts into nude mice (Fig. 5A). Tumour volume



and weight were measured. Mean tumour volumes and weights ( $387.4 \pm 23.5 \text{ mm}^3$  and  $531 \pm 27 \text{ mg}$ , respectively) at day 50 in mice receiving *HOTAIR*-overexpressing SiHa cells were significantly larger than those ( $309.3 \pm 32.7 \text{ mm}^3$  and  $380 \pm 93 \text{ mg}$ , respectively) in mice receiving empty vector-expressing cells ( $P < 0.001$ ) (Fig. 5B). *HOTAIR* expressions in tumor tissue were significantly higher in *HOTAIR*-overexpressing cells than those in control (Fig. 5C, 5D). Tumour weight correlated with tumour volume, as determined by callipers ( $P < 0.001$ ;  $r^2 = 0.935$ ). Histological examination revealed that more cells with large nucleoli and irregular nuclear membranes were present in *HOTAIR*-overexpressing xenografts than in control xenografts (Fig. 5E). We further evaluated tumour size and activity by Magnetic Resonance Imaging (MRI) and Positron Emission Tomography (PET) (Fig. 5F, 5G). Tumour growth was strongly induced by *HOTAIR* overexpression; tumour size and fluorodeoxyglucose (FDG) accumulation were significantly higher in mice inoculated with *HOTAIR*-overexpressing cells than empty vector-expressing cells. These findings suggest that *HOTAIR* can promote tumour growth *in vivo* and further support our initial hypothesis that *HOTAIR* plays a functional role in the malignant transformation of cervical cancer cells.

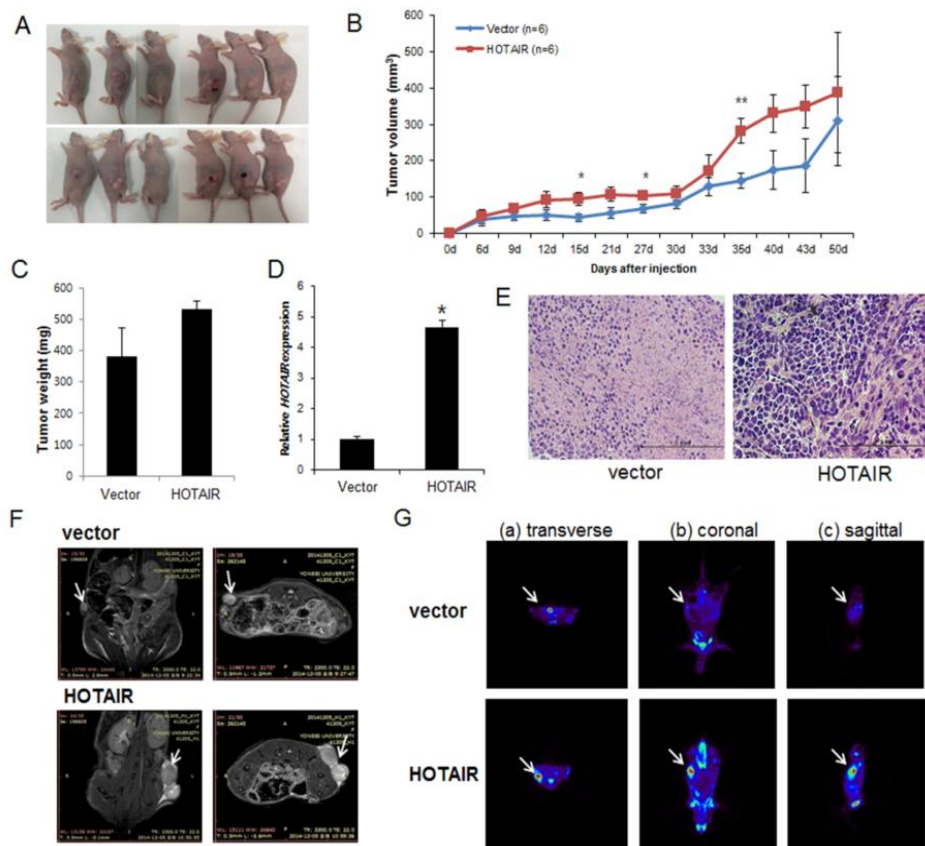


**Figure 5. Effect of *HOTAIR* on tumor growth *in vivo***

(A) SiHa cells ( $5 \times 10^6$ ) stably expressing *HOTAIR* were inoculated into nude mice, and the effect of *HOTAIR* on cervical tumour growth was examined after 50 days ( $n = 6$ ). A photograph of the tumours is presented. (B) Tumour volume was calculated every 3 days. Data are mean  $\pm$  SD ( $n = 6$ ). \* $P < 0.05$  and \*\* $P < 0.001$  vs. control. (C) Tumour weight. Data are mean  $\pm$  SD. (D) qRT-PCR analysis of *HOTAIR* expression in tissues of resected tumours. (E) Haematoxylin and eosin staining at 50 days after injection. (F) MRI imaging. (G) Micro PET image with transverse (a), coronal (b), and sagittal (c) plane slices of mice showing FDG uptake in the affected right carotid artery (arrows).

## **6. *HOTAIR* promotes a malignant phenotype in cervical cancer cells through the epithelial-mesenchymal transition (EMT) and Notch signalling pathways**

To determine the mechanism by which *HOTAIR* promotes a malignant phenotype in cervical cells, we assessed the status of important signalling cascades controlled by Notch in *HOTAIR*-overexpressing cells. *HOTAIR* overexpression in SiHa cells led to an increase in NOTCH1, HES1, and p300 expression at both the RNA (Fig. 6A) and protein (Fig. 6B, 6C) levels.

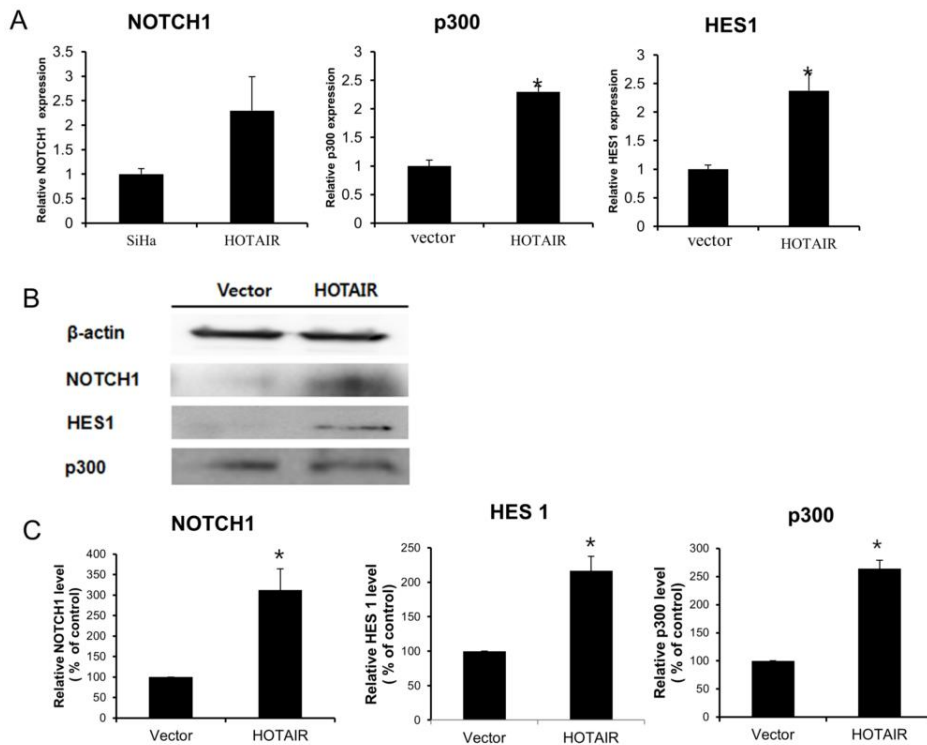


**Figure 6. *HOTAIR* regulates the Notch signalling pathway**

(A) *NOTCH1*, *p300*, and *HES1* levels were determined by qRT-PCR in *HOTAIR*-overexpressing SiHa cells. Each assay was performed in triplicate. Data are mean  $\pm$  SD. \* $P < 0.05$  vs. control. (B) Protein lysates were obtained from *HOTAIR*-overexpressing SiHa cells. *NOTCH1*, *p300*, and *HES1* expression levels were analysed by western blotting. (C) Band intensities were quantified and normalized to that of  $\beta$ -actin.

Next, we determined the expression of EMT-related genes and *NOTCH1* levels in xenografts derived from *HOTAIR*-overexpressing SiHa cells. As shown in Fig. 7, the expression of  $\beta$ -catenin, N-cadherin, Vimentin, Snail, and Twist was higher in *HOTAIR*-overexpressing tumours than in control tumours.

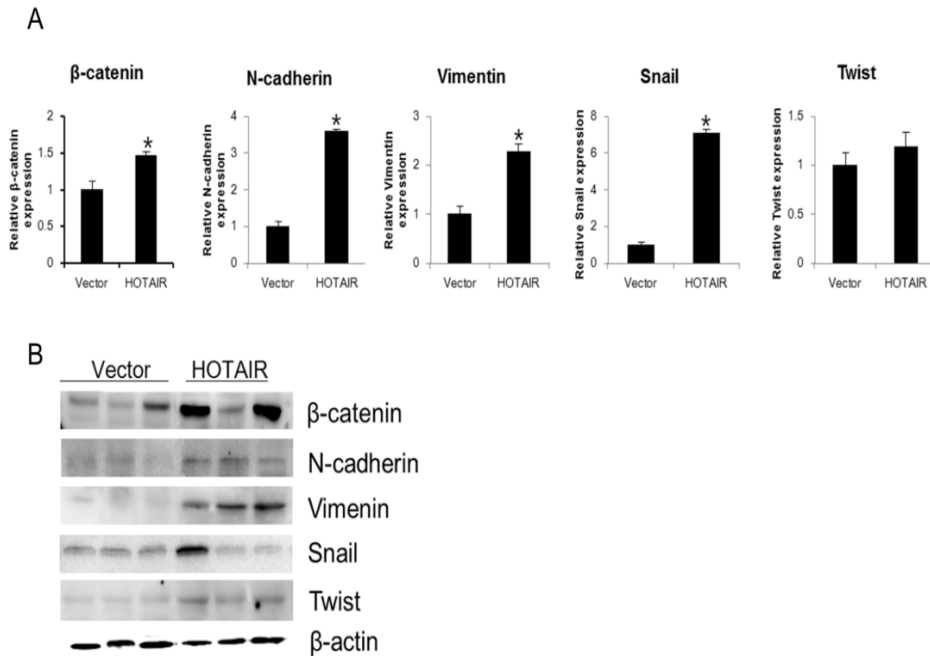


**Figure 7. *HOTAIR* overexpression promotes EMT-related gene expression in xenografts**

$\beta$ -catenin, N-cadherin, Vimentin, Snail, and Twist expression was analysed by qRT-PCR (A) and western blotting (B). Each assay was performed in triplicate. Data are mean  $\pm$  SD. \* $P < 0.05$  vs. control.

We also examined the expression of *NOTCH1*, *HES1*, and *p300* by qRT-PCR in xenografts derived from *HOTAIR*-overexpressing SiHa cells (Fig. 8A, 8B). *NOTCH1*, *HES1*, and *p300* expression was significantly higher in

*HOTAIR*-overexpressing xenograft tumours. These findings suggest that *HOTAIR* can promote tumour growth *in vivo* through the EMT and Notch signalling pathways.

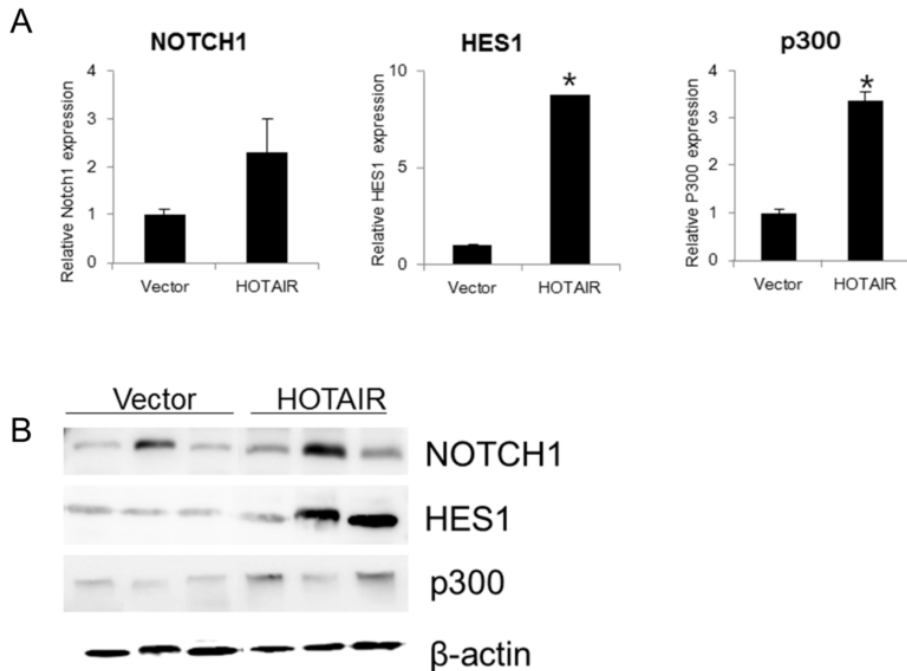


**Figure 8. *HOTAIR* overexpression promotes the expression of Notch pathway genes in xenografts**

(A) The expression of *NOTCH1*, *HES1*, and *p300* was determined by qRT-PCR in xenografts derived from *HOTAIR*-overexpressing SiHa cells. Each assay was performed in triplicate. Data are mean  $\pm$  SD. \* $P < 0.05$  vs. control. (B) Protein lysates were obtained from *HOTAIR* expression in tissues of resected tumors. *NOTCH1*, *HES1* and *p300* expression were analyzed by western blotting.

#### IV. DISCUSSION

In addition to identifying novel diagnostic markers for cervical cancer, a further understanding of the molecular mechanisms underlying the progression and metastasis of cervical cancer is needed to develop more effective therapeutic treatments. Among various genes and proteins previously identified to be overexpressed or modified in cervical cancer, the *HOTAIR* lncRNA has attracted research interest due to its marked and consistent overexpression in all cell lines and its reported role in cell growth and survival in other cancers.<sup>16</sup> In the present study, we investigated the functional role and clinical significance of circulating *HOTAIR* in cervical cancer using patient serum, cervical cancer cell lines, and mouse xenograft models.

*HOTAIR* expression was higher in tumours with nodal metastasis than in non-nodal metastatic tumours. Notably, high *HOTAIR* status and lymphatic invasion were prognostic factors for both disease-free and overall survival. Taken together, these results suggest that *HOTAIR* may play an important role in the pathogenesis of cervical cancer. However, it should be noted that our relatively small clinical sample size is a limitation of this study and may weaken the strength of our clinical analysis.

From a clinical point of view, the serum lncRNA signature for cervical cancer may be also useful for identifying cervical cancer progression. Although no significant difference was observed when the cervical cancer cases were stratified by age, histological tumour type, or SCC Ag levels, we identified a clear correlation between serum *HOTAIR* expression and tumour size, LVSI, and LN metastasis in cervical cancer. These results indicate that a high expression level of serum *HOTAIR* is associated with advanced disease status in cervical cancer patients.

*HOTAIR* targets HOX genes and binds to PRC2 and targets the repressive PRC2 complex to different genomic sites PRC<sup>8,9,17,18</sup> and is related to the initiation and progression of many cancer types.<sup>19-22</sup> In cervical cancer, *HOTAIR*

is related to tumour stage and EMT and is associated with poor prognosis.<sup>10,11</sup> Increasing evidence suggests a critical role for *HOTAIR* in cell growth, invasion, cancer metastasis, EMT, and stemness.<sup>23,34</sup> We therefore investigated the potential roles of *HOTAIR* in cervical cancer based on our prior analysis of clinical specimens. *HOTAIR* overexpression resulted in significant increases in cell proliferation and clonogenicity. Conversely, *HOTAIR* knockdown led to the suppression of these phenotypes and increased apoptosis. Importantly, *HOTAIR* overexpression positively correlated with cell migration and invasion in cervical cancer cell *in vitro* cultures and with tumour growth *in vivo* in xenograft-bearing mice. Our findings suggest that *HOTAIR* is one of the critical lncRNAs contributing to cervical cancer carcinogenesis and progression.

Previous studies reported that Notch1 signalling contributes to features of tumour progression, such as invasion, EMT, metastasis, and angiogenesis.<sup>25,26</sup> Notch1 induces anoikis resistance, inhibits p53 activity and upregulates Myc in cervical carcinoma and also inhibits the growth inhibitory effects of TGF- $\beta$  during cell growth.<sup>27-29</sup> Our earlier report suggests that EMT in cervical cancer correlates with *HOTAIR* expression.<sup>10</sup> Although there is data supporting the role of Notch1 in tumour progression, there is a paucity of evidence of factors downstream of it that regulates these processes associated with *HOTAIR*.

Finally, we investigated whether the EMT and Notch-Wnt signalling pathways are compromised upon *HOTAIR* overexpression or knockdown. There was an obvious relationship between increased levels of EMT-related genes, *NOTCH1*, *HES1*, *p300* and overexpression of *HOTAIR* in SiHa cells. Conversely, *HOTAIR* knockdown decreased the expression of EMT-related genes in HeLa cells. Thus, *HOTAIR* may contribute to the malignant phenotype of cervical cancer cells through the activation of Wnt-Notch signalling and EMT.



## V. CONCLUSION

In summary, we demonstrate that serum *HOTAIR* expression was low in normal cervical epithelium, and high in cervical cancer. Enhanced serum *HOTAIR* expression correlated positively with clinicopathological parameters in both *in vitro* and *in vivo* cervical cancer cells, lending support for the use of *HOTAIR* to determine clinicopathological stage and/or prognosis in cervical cancer. In addition, *HOTAIR* could be a potential therapeutic target, as the present study demonstrated the mechanistic role of *HOTAIR* in promoting cell motility and invasion through the Notch-Wnt signaling pathway and EMT.

## REFERENCES

1. Ferlay J, Soerjomataram I, Dikshit R, Eser S, Mathers C, Rebelo M, et al. Cancer incidence and mortality worldwide: Sources, methods and major patterns in GLOBOCAN 2012. *Int J Cancer* 2015, 136(5):E359-86.
2. Siegel R, Naishadham D, Jemal A: Cancer statistics, 2013. *CA Cancer J Clin* 2013, 63(1):11-30.
3. Schwarzenbach H, Hoon DSB, Pantel K: Cell-free nucleic acids as biomarkers in cancer patients. *Nat Rev Cancer* 2011, 11(6):426-37.
4. Crowley E, Di Nicolantonio F, Loupakis F, Bardelli A: Liquid biopsy: monitoring cancer-genetics in the blood. *Nat Rev Clin Oncol* 2013, 10(8):472-84.
5. Ren SC, Wang FB, Shen J, Sun Y, Xu WD, Lu J, et al: Long non-coding RNA metastasis associated in lung adenocarcinoma transcript 1 derived miniRNA as a novel plasma-based biomarker for diagnosing prostate cancer. *Eur J Cancer* 2013, 49(13):2949-59.
6. Koh W, Pan WY, Gawad C, Fan HC, Kerchner GA, Wyss-Coray T, et al: Noninvasive in vivo monitoring of tissue-specific global gene expression in humans. *P Natl Acad Sci USA* 2014, 111(20):7361-66.
7. Lee GL, Dobi A, Srivastava S: Prostate cancer: diagnostic performance of the PCA3 urine test. *Nat Rev Urol* 2011, 8(3):123-4.
8. Rinn JL, Kertesz M, Wang JK, Squazzo SL, Xu X, Brugmann SA, et al: Functional demarcation of active and silent chromatin domains in human HOX loci by Noncoding RNAs. *Cell* 2007, 129(7):1311-23.
9. Gupta RA, Shah N, Wang KC, Kim J, Horlings HM, Wong DJ, et al: Long non-coding RNA HOTAIR reprograms chromatin state to promote cancer metastasis. *Nature* 2010, 464(7291):1071-U1148.
10. Kim HJ, Lee DW, Yim GW, Nam EJ, Kim S, Kim SW, et al: Long

- non-coding RNA HOTAIR is associated with human cervical cancer progression. *Int J Oncol* 2015, 46(2):521-30.
11. Huang L, Liao LM, Liu AW, Wu JB, Cheng XL, Lin JX, et al: Overexpression of long noncoding RNA HOTAIR predicts a poor prognosis in patients with cervical cancer. *Arch Gynecol Obstet* 2014, 290(4):717-23.
  12. Chen X, Ba Y, Ma L, Cai X, Yin Y, Wang K, et al: Characterization of microRNAs in serum: a novel class of biomarkers for diagnosis of cancer and other diseases. *Cell Res* 2008, 18(10):997-1006.
  13. Mitchell PS, Parkin RK, Kroh EM, Fritz BR, Wyman SK, Pogosova-Agadjanyan EL, et al: Circulating microRNAs as stable blood-based markers for cancer detection. *P Natl Acad Sci USA* 2008, 105(30):10513-18.
  14. Ng EKO, Chong WWS, Jin H, Lam EKY, Shin VY, Yu J, et al: Differential expression of microRNAs in plasma of patients with colorectal cancer: a potential marker for colorectal cancer screening. *Gut* 2009, 58(10):1375-81.
  15. Resnick KE, Alder H, Hagan JP, Richardson DL, Croce CM, Cohn DE: The detection of differentially expressed microRNAs from the serum of ovarian cancer patients using a novel real-time PCR platform. *Gynecol Oncol* 2009, 112(1):55-9.
  16. Hajjari M, Salavaty A: HOTAIR: an oncogenic long non-coding RNA in different cancers. *Cancer Biol Med* 2015, 12(1):1-9.
  17. Hajjari M, Khoshnevisan A, Shin YK: Molecular function and regulation of long non-coding RNAs: paradigms with potential roles in cancer. *Tumour Biol* 2014, 35(11):10645-63.
  18. Cifuentes-Rojas C, Hernandez AJ, Sarma K, Lee JT: Regulatory Interactions between RNA and Polycomb Repressive Complex 2. *Mol Cell* 2014, 55(2):171-85.

19. Nie Y, Liu X, Qu SH, Song EW, Zou H, Gong C: Long non-coding RNA HOTAIR is an independent prognostic marker for nasopharyngeal carcinoma progression and survival. *Cancer Sci* 2013, 104(4):458-64.
20. Chiyomaru T, Fukuhara S, Saini S, Majid S, Deng GR, Shahryari V, et al: Long Non-coding RNA HOTAIR Is Targeted and Regulated by miR-141 in Human Cancer Cells. *J Biol Chem* 2014, 289(18):12550-65.
21. Cai B, Wu ZJ, Liao K, Zhang S: Long noncoding RNA HOTAIR can serve as a common molecular marker for lymph node metastasis: a meta-analysis. *Tumor Biol* 2014, 35(9):8445-50.
22. Endo H, Shiroki T, Nakagawa T, Yokoyama M, Tamai K, Yamanami H, et al: Enhanced Expression of Long Non-Coding RNA HOTAIR Is Associated with the Development of Gastric Cancer. *Plos One* 2013, 8(10).
23. Alves CP, Fonseca AS, Muys BR, Bueno RDEL, Burger MC, de Souza JES, et al: Brief Report: The lincRNA Hotair Is Required for Epithelial-to-Mesenchymal Transition and Stemness Maintenance of Cancer Cell Lines. *Stem Cells* 2013, 31(12):2827-32.
24. Sorensen KP, Thomassen M, Tan QH, Bak M, Cold S, Burton M, et al: Long non-coding RNA HOTAIR is an independent prognostic marker of metastasis in estrogen receptor-positive primary breast cancer. *Breast Cancer Res Tr* 2013, 142(3):529-36.
25. Timmerman LA, Grego-Bessa J, Raya A, Bertran E, Perez-Pomares JM, Diez J, et al: Notch promotes epithelial-mesenchymal transition during cardiac development and oncogenic transformation. *Genes Dev* 2004, 18(1):99-115.
26. Wang Z, Banerjee S, Li Y, Rahman KM, Zhang Y, Sarkar FH: Down-regulation of notch-1 inhibits invasion by inactivation of nuclear factor-kappaB, vascular endothelial growth factor, and matrix

- metalloproteinase-9 in pancreatic cancer cells. *Cancer Res* 2006, 66(5):2778-84.
27. Nair P, Somasundaram K, Krishna S: Activated Notch1 inhibits p53-induced apoptosis and sustains transformation by human papillomavirus type 16 E6 and E7 oncogenes through a PI3K-PKB/Akt-dependent pathway. *J Virol* 2003, 77(12):7106-12.
28. Klinakis A, Szaboics M, Politi K, Kiaris H, Artavanis-Tsakonas S, Efstratiadis A: Myc is a Notch1 transcriptional target and a requisite for Notch1-induced mammary tumorigenesis in mice. *P Natl Acad Sci USA* 2006, 103(24):9262-7.
29. Masuda S, Kumano K, Shimizu K, Imai Y, Kurokawa M, Ogawa S, et al: Notch1 oncoprotein antagonizes TGF-beta/Smad-mediated cell growth suppression via sequestration of coactivator p300. *Cancer Sci* 2005, 96(5):274-82.

< ABSTRACT (IN KOREAN) >

자궁경부암에서 혈청 바이오마커로 Notch 신호경로를 통한 긴 비 암호화 RNA인 *HOTAIR*의 개발

<지도교수 김영태>

연세대학교 대학원 의학과

이마리아

**목적:** 본 연구의 목적은 자궁경부암 환자 혈청에서 높게 측정되는 긴 비 암호화 RNA를 발견하고, 이를 바탕으로 혈청 바이오마커를 개발하는 것이다. 그러한 물질 중의 *HOTAIR*의 자궁경부암 발생 과정에서의 역할을 알아 보고자 하였다.

**방법:** 153명의 자궁경부암 환자 혈청에서 *HOTAIR*의 발현을 측정하였다. 또한 lentivirus 기법을 이용하여 *HOTAIR* 과발현 세포를 확립하고 *HOTAIR*의 자궁경부암 암화과정에서의 역할을 연구 하였다.

**결과:** *HOTAIR* 발현이 자궁경부암 세포와 자궁경부암 환자 혈청에서 증가되어 있음을 확인 하였다. *HOTAIR*의 발현은 종양크기, 림프-혈관계 침범, 림프절 전이와 같은 예후 인자와 양의 상관관계를 보였으며 ( $P<0.05$ ), 단변량 생존분석에서 *HOTAIR* 과발현은 자궁경부암의 생존에 관련된 예후 인자였다. 자궁경부암 세포주를 이용한 기능 연구 결과 *HOTAIR*가 세포 증식과 사멸, 종양 형성, 세포 이동 및 침습에 NOTCH 신호전달경로를 매개하여 중요한 역할을 하고 있음을 확인하였다.

**결론:** 본 연구는 *HOTAIR*가 자궁경부암 혈청 바이오마커로 의미를 가지며, 자궁경부암의 암화과정에 중요한 역할을 하고 있고 자궁경부암 표적치료의 새로운 표지자로서의 가능성이 있음을 보여주었다.

---

핵심되는 말: 자궁경부암; 긴 비 암호화 RNA; *HOTAIR*; lentivirus; Notch